3. Zipes DP. The long QT interval syndrome: a Rosetta stone for sympathetic related ventricular tachyarrhythmias. Circulation 1991; 84:1414–1419.

4. Roden DM, Lazzara R, Rosen MR, Schwartz PJ, Towbin JA, Vincent GM, Antzelevitch C, Brown AM, Colatsky TJ, Crampton RS, Kass RS, Moss AJ, Sanguinetti MC, Zipes DP.The SADS Foundation Task Force on LQTS Multiple mechanisms in the long-QT syndrome: current knowledge, gaps, and future directions. Circulation 1996;94:1996–2012.

5. Wilde AAM, Jongbloed RJE, Doevendans PA, Duren DR, Hauer RNW, van Langen IM, van Tintelen JP, Smeets HJM, Meyer H, Geelen JLMC. Auditory stimuli as a trigger for arrhythmic events differentiate HERG-related (LQT2) patients from KVLQT1–related patients (LQT1). J Am Coll Cardiol 1999;33:327–332.

6. Moss AJ, Robinson JL, Gessman L, Gillespie R, Zareba W, Schwartz P J, Vincent GM, Benhorin J, Locati Heilbron E, Towbin JA, Priori SG, Napolitano C, Zhang L, Medina A, Andrews ML, Timothy K. Comparison of clinical and genetic variables of cardiac events associated with loud noise versus swimming among subjects with the long QT syndrome. Am J Cardiol 1999;84:876–879.

7. Ackerman MJ, Tester DJ, Porter CJ, Edwards WD. Molecular diagnosis of the inherited long-QT syndrome in a woman who died after near-drowning. N Engl J Med 1999;341:1121–1125.

8. Schwartz PJ, Priori SG, Spazzolini C, Moss AJ, Vincent GM, Napolitano C, Denjoy I, Guicheney P, Breithardt G, Keating MT, Towbin JA, Beggs AH, Brink P, Wilde AA, Toivonen L, Zareba W, Robinson JL, Timothy KW, Corfield V, Wattanasirichaigoon D, Corbett C, Haverkamp W, Schulze-Bahr E, Lehmann MH, Schwartz K, Coumel P, Bloise R. Genotype-phenotype correlation in the long-QT syndrome: gene-specific triggers for life-threatening arrhythmias. Circulation 2001;103:89–95.

9. Dorostkar PC, Eldar M, Belhassen B, Scheinman MM. Long-term follow-up of patients with long-QT syndrome treated with beta-blockers and continuous pacing. Circulation 1999;100:2431–2436.

10. Moss AJ, Zareba W, Hall WJ, Schwartz PJ, Crampton RS, Benhorin J, Vincent GM, Locati EH, Priori SG, Napolitano C, Medina A, Zhang L, Robinson JL, Timothy K, Towbin JA, Andrews ML. Effectiveness and limitations of beta-blocker therapy in congenital long-QT syndrome. Circulation 2000;101:616–623.

11. Zareba W, Moss AJ, Schwartz PJ, Vincent GM, Robinson JL, Priori SG, Benhorin J, Locati EH, Towbin JA, Keating MT, Lehmann MH, Hall WJ. Influence of the genotype on the clinical course of the long-QT syndrome. N Engl J Med 1998;339:960–965.

12. Noda T, Takaki H, Kurita T, Suyama K, Nagaya N, Taguchi A, Aihara N, Kamakura S, Sunagawa K, Nakamura K, Ohe T, Horie M, Napolitano C, Towbin J A, Priori SG, Shimizu W. Gene-specific response of dynamic ventricular repolarization to sympathetic stimulation in LQT1, LQT2 and LQT3 forms of congenital long QT syndrome. Eur Heart J 2002;23:975–983.

13. Ackerman MJ, Khositseth A, Tester DJ, Hejlik JB, Shen WK, Porter CB. Epinephrine-induced QT interval prolongation: a gene-specific paradoxical response in congenital long QT syndrome. Mayo Clin Proc 2002;77:413–421.

14. Shimizu W, Tanabe Y, Aiba T, Inagaki M, Kurita T, Suyama K, Nagaya N, Taguchi A, Aihara N, Sunagawa K, Nakamura K, Ohe T, Towbin JA, Priori SG, Kamakura S. Differential effects of beta-blockade on dispersion of repolarization in absence and presence of sympathetic stimulation between LQT1 and LQT2 forms of the long QT syndrome.

15. Keating M, Atkinson D, Dunn C, Timothy K, Vincent GM, Leppert M. Linkage of a cardiac arrhythmia, the long QT syndrome, and the Harvey ras-1 gene. Science 1991;252:704–706.

16. Schwartz PJ, Moss AJ, Vincent GM, Crampton RS. Diagnostic criteria for the long QT syndrome: an update. Circulation 1993;88: 782–784.

17. Moss AJ, Schwartz PJ, Crampton RS, Tzivoni D, Locati EH, MacCluer JW, Hall WJ, Weitkamp LR, Vincent GM, Garson A, Robinson JL, Benhorin J, Choi S. The long QT syndrome: prospective longitudinal study of 328 families. Circulation 1991;84:1136–1144.

18. Vincent GM, Timothy KW, Leppert M, Keating MT. The spectrum of symptoms and QT intervals in carriers of the gene for the long-QT syndrome. N Engl J Med 1992;327:846–852.

19. Priori SG, Napolitano C, Schwartz PJ. Low penetrance in the long-QT syndrome: clinical impact. Circulation 1999;99:529–533.

20. Swan H, Saarinen K, Kontula K, Toivonen L, Viitasalo M. Evaluation of QT interval duration and dispersion and proposed clinical criteria in diagnosis of long QT syndrome in patients with a genetically uniform type of LQT1. J Am Coll Cardiol 1998;32:486–491.

21. Shimizu W, Antzelevitch C. Cellular basis for the electrocardiographic features of the LQT1 form of the long QT syndrome: effects of beta-adrenergic agonists, antagonists and sodium channel blockers on transmural dispersion of repolarization and torsade de pointes. Circulation 1998;98:2314–2322.

22. Antzelevitch C, Yan G X, Shimizu W, Burashnikov A. Electrical heterogeneity, the ECG, and cardiac arrhythmias. In: Zipes DP, Jalife J, eds. Cardiac electrophysiology: from cell to bedside, 3rd ed. Philadelphia: WB Saunders, 1999:222–238..

23. Shimizu W, Antzelevitch C. Differential response to beta-adrenergic agonists and antagonists in LQT1, LQT2 and LQT3 models of the long QT syndrome. J Am Coll Cardiol 2000;35:778–786.

24. Splawski I, Shen J, Timothy KW, Lehmann MH, Priori S, Robinson JL, Moss AJ, Schwartz PJ, Towbin JA, Vincent GM, Keating MT. Spectrum of mutations in long-QT syndrome genes: KVLQT1, HERG, SCN5A, KCNE1, and KCNE2. Circulation 2000;102:1178–1185.

25. Zhang L, Timothy KW, Vincent GM, Lehmann MH, Fox J, Giuli LC, Shen J, Splawski I, Priori SG, Compton SJ, Yanowitz F, Benhorin J, Moss AJ, Schwartz PJ, Robinson JL, Wang Q, Zareba W, Keating MT, Towbin JA, Napolitano C, Medina A. Spectrum of ST-T-wave patterns and repolarization parameters in congenital long-QT syndrome: ECG findings identify genotypes. Circulation 2000;102:2849–2855.

26. Lupoglazoff JM, Denjoy I, Berthet M, Neyroud N, Demay L, Richard P, Hainque B, Vaksmann G, Klug D, Leenhardt A, Maillard G, Coumel P, Guicheney P. Notched T waves on holter recordings enhance detection of patients with LQT2 (HERG) mutations. Circulation 2001;103:1095–1101.

27. Viitasalo M, Oikarinen L, Swan H, Vaananen H, Glatter K, Laitinen PJ, Kontula K, Barron HV, Toivonen L, Scheinman MM. Ambulatory electrocardiographic evidence of transmural dispersion of repolarization in patients with long-QT syndrome type 1 and 2. Circulation 2002;106:2473–2478.

28. Takenaka K, Ai T, Shimizu W, Kobori A, Ninomiya T, Otani H, Kubota T, Takaki H, Kamakura S, Horie M. Exercise stress test amplifies genotype-phenotype correlation in the LQT1 and LQT2 forms of the long QT syndrome. Circulation 2003;107:838–844.

Acetylcholine From Vagal Stimulation Protects Cardiomyocytes Against Ischemia and Hypoxia Involving Additive Nonhypoxic Induction of HIF-1α

Yoshihiko Kakinuma, Motonori Ando, *Masanori Kuwabara, Rajesh G. Katare,
#Koji Okudela, +Masanobu Kobayashi, Takayuki Sato

Department of Cardiovascular Control, *Department of Medicine and Geriatrics,
Kochi Medical School, Nankoku, Japan.
#Department of Pathology, Division of Cellular Pathobiology,
Yokohama City University Graduate School of Medicine, Yokohama, Japan.
+Division of Cancer Pathobiology, Institute for Genetic Medicine, Hokkaido University, Sapporo, Japan

Correspondence:Yoshihiko Kakinuma, M.D., Ph.D. Department of Cardiovascular Control Kochi Medical SchoolNankoku,
783-8505, Japan
FAX: +81-88-880-2310   TEL:+81-88-880-2587   E-mail:kakinuma@med.kochi-u.ac.jp

ABSTRACT
Electrical stimulation of the vagal efferent nerve improves the survival of myocardial infarcted rats. However, the mechanism for this beneficial effect is unclear. We investigated the effect of acetylcholine (ACh) on HIF-1α using rat cardiomyocytes under normoxia and hypoxia. ACh posttranslationally regulated HIF-1α and increased its protein level under normoxia. ACh increased Akt phosphorylation, and wortmannin or atropine blocked this effect. Hypoxia-induced caspase-3 activation and mitochondrial membrane potential collapse were prevented by ACh. Dominant-negative HIF-1α inhibited the cell protective effect of ACh. In acute myocardial ischemia, vagal nerve stimulation increased HIF-1α expression and reduced the infarct size. These results suggest that ACh and vagal stimulation protect cardiomyocytes through the PI3K/Akt/HIF-1α pathway.

Key words: acetylcholine, ischemia, apoptosis, protein kinases

1. Introduction
The prognosis of patients with chronic heart failure remains poor, due to progressive remodeling of the heart and lethal arrhythmia. Acute ischemia or hypoxia causes loss of cardiomyocytes, followed by remodeling in the chronic phase. Although various therapeutic approaches have been introduced, including implantable defibrillators [1], a more effective modality of therapy has been anticipated for several years. A recent animal study by Li et al. demonstrated that vagal nerve stimulation prevented ventricular remodeling after myocardial infarction, suggesting a novel therapeutic strategy against heart failure [2]. Furthermore, Krieg et al. reported that acetylcholine (ACh) has a cardioprotective effect [3]. Although nitric oxide (NO) is supposed to be a major signaling molecule induced by ACh, a mechanism for the beneficial effect of vagal nerve stimulation on cardiomyocytes remains to be clarified. To investigate this mechanism, we hypothesized that vagal stimulation or ACh directly triggers a cell survival signal that is subsequently amplified and leads to protection of the cardiomyocytes from acute ischemic conditions, and that this effect of ACh, if continued, could be responsible for chronic cardioprotection.

In the present study, we focused on demonstrating the cellular action of ACh through hypoxia-inducible factor (HIF)-1α. HIF-1α is a transcription factor that is important for cell survival under hypoxia. HIF-1α activates the expression of many genes indispensable for cell survival [4,5]. Under normoxia, the HIF-1α protein level is very low, due to proteasomal degradation through with von Hippel-Lindau tumor suppressor protein (VHL). However, HIF-1α escapes from this degradation under hypoxia, and this is recognized as the hypoxic pathway [6,7]. Recently, it was revealed that HIF-1α can be also induced via a nonhypoxic pathway by angiotensin II [8,9]. Taken together, it is conceivable that HIF-1α induction is one of the adaptation processes to hypoxia and ischemia, and that additional induction of HIF-1α during ischemia via a nonhypoxic pathway could provide further cardioprotection.

Therefore, we investigated the direct effects of ACh on survival signaling in cardiomyocytes and of vagal stimulation on hearts. The results suggest that ACh and vagal stimulation protect cardiomyocytes from acute hypoxia and ischemia via additional HIF-1α protein induction through a nonhypoxic pathway.

2. Materials and Methods
2.1. Cell Culture
To examine the effect of ACh on cardiomyocytes, H9c2 cells as well as primary cardiomyocytes isolated from neonatal rats were used. H9c2 cells, which are frequently used to investigate signal

transduction and channels in rat cardiomyocytes, are derived from rat embryonic ventricular cardiomyocytes. H9c2 cells were incubated in DMEM containing 10% FBS and antibiotics. Primary cardiomyocytes were isolated from 2-3-day-old neonatal WKY rats and incubated in DMEM/Ham F-12 containing 10% FBS. HEK293 cells and HeLa cells cultured in DMEM containing 10% FBS were also used.

2.2. Western Blot Analysis

H9c2 cells and primary cardiomyocytes were treated with 1 mM ACh to evaluate expression of HIF-1a protein under normoxia or with 1 mM S-nitroso-N-acetylpenicillamine (SNAP) to study the signal transduction. To investigate the signal transduction, H9c2 cells were pretreated with a PI3K inhibitor, (wortmannin; 300 nM), a muscarinic receptor, (atropine; 1 mM), a transcriptional inhibitor, (actinomycin D; 0.5 μg/ml) or a protein synthesis inhibitor, (cycloheximide; 10 μg/ml), followed by ACh treatment. Cell lysates were mixed with a sample buffer, fractionated by 10% SDS-PAGE and transferred onto membranes. The membranes were incubated with primary antibodies against HIF-1a (Santa Cruz Biotechnology, Santa Cruz, California, USA), Akt and phospho-Akt (Cell Signaling Technology, Beverly, Massachusetts, USA), and α-tubulin (Lab Vision, Fremont, California, USA), and then reacted with an HRP-conjugated secondary antibody (BD Transduction Laboratories, San Diego, California, USA). Positive signals were detected with an enhanced chemiluminescence system (Amersham, Piscataway, New Jersey, USA). In each study, the experiments were performed in duplicate and repeated 3-5 times (n=3-5). Representative data are shown.

2.3. MTT Activity Assay

To evaluate the effects of hypoxia and ACh on the mitochondrial function of cardiomyocytes, we measured 3-(4,5-dimethylthiazol-2-yl)-2,5-diphenyl tetrazolium bromide (MTT) reduction activity in H9c2 or HEK293 cells under hypoxia (1% oxygen concentration), in the presence or absence of ACh. The cells were pretreated with 1 mM ACh for 12 hours, and then subjected to hypoxia for 12 hours. At 4 hours before sampling, the MTT reagents were added to the culture and incubated.

2.4. Caspase-3 Activity Assay

Caspase-3 activity was measured using a CPP32/Caspase-3 Fluorometric Protease Assay Kit, (CHEMICON INTERNATIONAL, Temecula, California, USA). Hypoxia-treated H9c2 cells with or without 1 mM ACh pretreatment were lysed and the cytosolic extract was added to the caspase-3 substrate. A fluorometer equipped with a 400-nm excitation filter and 505-nm emission filter was used to measure the samples.

2.5. DePsipher Assay

To examine the effects of hypoxia and ACh on the mitochondrial electrochemical gradient, we analyzed cardiomyocytes using a DePsipher™ Mitochondrial Potential Assay Kit (Trevigen, Gaithersburg, Maryland, USA). Apoptotic cells, which undergo mitochondrial membrane potential collapse cannot accumulate the DePsipher reagent in their mitochondria. As a result, apoptotic cells show decreased red fluorescence in their mitochondria, and the reagent remains in the cytoplasm as a green fluorescent monomer. Therefore, apoptotic cells were easily differentiated from healthy cells, which showed more red fluorescence.

2.6. Evaluation of NO production

NO production was measured using the 4,5 diaminofluoresceindiacetate (DAF-2DA; Alexis, Lausen, Switzerland) fluorometric NO detection system as previously reported [10]. The intensity of the DAF-2DA green fluorescence in ACh-treated cells was measured and compared with that in non-treated cells (λ Ex. 492 nm; λ Em. 515 nm).

2.7. Transfection

To investigate the direct contribution of Akt phosphorylation to HIF-1a stabilization or that of HIF-1a to the ACh effect, HEK293 cells were transfected with an expression vector for wild-type Akt (wt Akt), dominant-negative Akt (dn Akt), wild-type HIF-1α (wt HIF-1α) or dominant-negative HIF-1α (dn HIF-1α), using Effectene (Qiagen, Valencia, California, USA) according to the manufacture's protocol. The Akt vectors were generous gifts from by Dr. K. Okudela (Yokohama City University, Kanagawa, Japan) [11], while the HIF-1α vectors were kindly provided by Dr. M. Kobayashi (Hokkaido University, Sapporo, Japan) [12]. After transfection, HEK293 cells were pretreated with 1 mM ACh for 12 hours, followed by evaluating the HIF-1α protein level or by hypoxia for 12 hours and MTT activity in each group was evaluated. As a control, cells were transfected with a vector for green fluorescent protein (GFP).

2.8. RT-PCR

Total RNA was isolated from H9c2 cells according to a modified acid guanidinium-phenol-chloroform method using an RNA isolation kit (ISOGEN; Nippon Gene, Tokyo, Japan), and reverse-transcribed to obtain a first-strand cDNA. This first-strand cDNA was amplified by specific primers for HIF-1a, and the PCR products were fractionated by electrophoresis.

2.9. Vagal Nerve Stimulation in Myocardial Ischemia

Left ventricular myocardial ischemia (MI) was performed by 3 hours of left coronary artery (LCA) ligation in anesthetized 9-week-old male Wistar rats

under artificial ventilation previously described [2]. Sham-operated (control) rats did not undergo LCA ligation. For vagal nerve stimulation (VS), the right vagal nerve in the neck was isolated and cut. Only the distal end of the vagal nerve was stimulated in order to exclude the effects of the vagal afferent. The electrode was connected to an isolated constant voltage stimulator. VS was performed from 1 min before the LCA ligation until 3 hours afterwards, using 0.1 ms pulses at 10 Hz (MI-VS). The electrical voltage of the pulses was adjusted to obtain a 10% reduction in the heart rate before LCA ligation, but VS (MI-VS) was not associated with any blood pressure reduction during the experiments, compared with MI. At the end of the experiments, the rats were either injected with 2 ml of 2% Evans blue dye via the femoral vein to measure the risk area followed by determination of the infarct size with 2% triphenyl tetrazolium chloride (TTC) staining or the heart was excised for protein isolation and subsequent western blotting to detect HIF-1a protein. The percentage of the infarcted area of the left ventricle (LV) was calculated as the ratio of the infarcted area to the risk area.

2.10. Densitometry
The western blotting data were analyzed using Kodak 1D Image Analysis Software (Eastman Kodak Co., Rochester, New York, USA).

2.11. Statistics
The data were presented as means ± S.E. The mean values between two groups were compared by the unpaired Student's t test. Differences among data were assessed by ANOVA for multiple comparisons of results. Differences were considered significant at $P < 0.05$.

3. Results
3.1. Posttranslational Regulation of HIF-1α by ACh through a Nonhypoxic Pathway
ACh (1 mM) increased HIF-1α protein expression in H9c2 cells under normoxia (Fig. 1A). ACh increased NO production, as evaluated by DAF-2DA (Figure 1B), suggesting that NO is involved in the signal transduction of HIF-1a induction. Actinomycin D (0.5 µg/ml; Figs. 2A, 2B) and cycloheximide (10 µg/ml; Fig. 2C) did not decrease the HIF-1α level under normoxia, suggesting that HIF-1α degradation is regulated by ACh. Furthermore, ACh increased HIF-1 α level in primary cardiomyocytes without reducing their beating rate (Fig. 3). Since H9c2 cells did not beat, these results suggest that HIF-1α induction is independent of the heart rate-decreasing effect of ACh.

3.2. Akt Phosphorylation by ACh
ACh had no effect on the total Akt protein level, but increased Akt phosphorylation (Fig. 4A) as effectively as SNAP (data not shown). The

ACh-induced Akt phosphorylation was inhibited by atropine in a dose-dependent manner (Fig. 4B). ACh-induced Akt phosphorylation and its inhibition by atropine were also observed in rat primary cardiomyocytes (Fig. 4C).

3.3. PI3K/Akt Pathway for HIF-1α induction by ACh
Wortmannin completely inhibited the ACh-induced Akt phosphorylation (Fig. 4D), in clear contrast to the data in Fig. 4A. Furthermore, it also attenuated the HIF-1α induction by ACh (Fig. 4E). To elucidate the contribution of Akt phosphorylation to HIF-1α protein level in normoxia, dn Akt was introduced into HEK293 cells, and found to partially inhibit the HIF-1α induction by ACh (Fig. 4F).

3.4. Effect of ACh on Apoptosis during Hypoxia
The DePsipher assay clearly showed that hypoxia (1% oxygen concentration) for 12 hours caused mitochondrial membrane potential collapse leading to cell death, and that 1 mM ACh inhibited this collapse in H9c2 cells (Fig. 5A). ACh attenuated the decrease in MTT activity caused by 12 hours of hypoxia in H9c2 cells (Fig. 5B; 103.4±0.8% in ACh+hypoxia vs. 56.6±0.7% in hypoxia, p<0.01, n=8) and HEK293 cells (p<0.01 vs. hypoxia). The caspase-3 activity was increased by hypoxia in H9c2 cells, and pretreatment with 1 mM ACh inhibited this increase (Fig. 5C; 128±2% in hypoxia vs. 90±2% in ACh+hypoxia, p<0.01, n=4). To elucidate the dependency of the ACh-induced protective effect on HIF-1α, dn HIF-1α was transfected into HEK293 cells, followed by ACh pretreatment and then hypoxia. It was found that dn HIF-1α inhibited the protective effect of ACh from hypoxia (Fig. 5D; 115.1±1.2% in wt HIF-1α and 111.8±1.8% in GFP vs. 59.0±3.4% in dn HIF-1α, p<0.05, n=10), suggesting that HIF-1α induction by ACh is partially responsible for the protective effect.

3.5. Effect of Vagal Stimulation on HIF-1a in Myocardial Ischemia
To evaluate the significance of ACh for cardioprotection in vivo, the vagal nerve was stimulated prior to the myocardial ischemia. Histological analysis demonstrated a tendency for the infarcted area from the vagal nerve-stimulated (MI-VS) hearts to be smaller than that from non-stimulated (MI) hearts (31.5±4.6% in MI-VS vs. 40.9±2.5% in MI, n=3), even though the risk areas (non-perfused areas) were comparable (Fig. 6A; 59.2±1.0% in MI-VS vs. 53.7±1.0% in MI, n=3). In the MI-VS hearts, the HIF-1α protein level was further elevated compared to that in the MI hearts (Fig. 6B; 244±24% in MI-VS vs. 112±1% in MI, n=3). These results suggest that vagal nerve stimulation in the ischemic heart activates both the hypoxic and nonhypoxic pathways of HIF-1α

induction, resulting in increased induction of HIF-1a.

3.6. Nonhypoxic Induction of HIF-1α in Other Cells

The observed ACh-mediated HIF-1α induction was not limited to H9c2 or primary cultured cardiomyocytes, but also found in several other types of cell lines, including HEK293, and HeLa cells (Figure 7). Since these cells did not beat spontaneously, the results suggest that the system of ACh-mediated HIF-1α induction is not only independent of the beating rate of cardiomyocytes, but also a generally conserved system in cells.

4. Discussion
Cardioprotective Action by ACh and Vagal Stimulation via the Muscarinic Receptor

Using animal models, several studies have shown that accentuated antagonism against the sympathetic nervous system is a major mechanism for the beneficial effect of vagal tone on the ischemic heart [13]. Although ACh was involved in triggering preconditioning mechanisms in an ischemia-reperfusion model [3], it remained unclear whether vagal nerve stimulation in acute ischemia or hypoxia followed these mechanisms. In the present study, we have disclosed that ACh possesses a protective effect on cardiomyocytes. In rat cardiomyocytes, ACh triggered a sequence of survival signals through Akt that eventually induced HIF-1α, inhibited the collapse of the mitochondrial membrane potential and decreased caspase-3 activity, thereby leading to the survival of cardiomyocytes under hypoxia. Furthermore, our results suggest ACh exerts this action through Akt in other cells. The current study therefore provides another insight into the cellular mechanism for the cardioprotective effects of ACh and vagal stimulation.

Signaling Pathway of ACh via PI3K/Akt and Antiapoptotic Effects of ACh

Since previous studies demonstrated that a PI3K inhibitor greatly reduced HIF-1α induction in heart and renal cells [14,15] and a few studies have reported that MAP kinase is activated through ACh, we focused on the PI3K/Akt pathway, one of the important cell survival signaling pathways [16], and found that ACh directly activated Akt phosphorylation via PI3K. PI3K/Akt signaling has been reported to have an antiapoptotic activity through various features, such as inhibition of Bad-binding to Bcl-2, caspase 9, Fas and glycogen synthetase kinase-3 [17,18]. These facts imply a definite involvement of Akt activation in cell survival. As shown using dn HIF-1α, ACh inhibited hypoxia-induced cell death through HIF-1α induction via Akt phosphorylation. These results indicate that ACh actually protects cardiomyocytes from hypoxia at the cellular level.

Additional Induction of HIF-1α by ACh and Vagal Stimulation

HIF-1α regulates the transcriptional activities of very diverse genes involved in cell survival and is itself regulated at the posttranslational level by VHL [4,6,7]. Recent studies have shown that HIF-1α is also regulated through a nonhypoxic pathway involving angiotensin II, TNF-α and NO [8,9,19,20]. Therefore, it is speculated that cardiomyocytes possess a similar system for regulating HIF-1α through ACh, independent of the oxygen concentration. Induction of HIF-1α is a powerful cellular response against hypoxia, and further increases in its expression by other pathways may be beneficial. The present results indicate that the significance of ACh or vagal nerve stimulation in hypoxic stress can be attributed to additional HIF-1α induction through dual induction pathways, i.e., hypoxic and nonhypoxic pathways.

The present study has revealed that ACh-mediated HIF-1α induction is widely conserved in other cells. Consistent with a previous report [10], the current results suggest that NO is produced by ACh. According to a report that NO attenuates the interaction between pVHL and HIF-1α through inhibiting PHD activity [21], it is possible that ACh may increase the HIF-1α protein level through NO. Recent studies conducted by Krieg et al. and Xi et al., have provided supportive data compatible with our results [3,22], while another study by Hirota et al. also revealed a nonhypoxic pathway for HIF-1α induction by ACh in a human kidney-derived cell line [23].

The signaling pathway of the muscarinic receptor has been studied extensively, and many pathways are involved in its specific biological effects. Therefore, possible involvement of other pathways in the nonhypoxic induction of HIF-1α cannot be excluded. However, it was demonstrated that dn Akt and dn HIF-1α decreased the effect of ACh. Consistent with a recent study [24], we have revealed that ACh or vagal stimulation protects cardiomyocytes in the acute phase. This observation suggests that the protective effect in the acute phase may result in inhibition of cardiac remodeling in the chronic phase, since vagal stimulation produces additional HIF-1α induction through a nonhypoxic pathway, which increases cell survival.

References
1. Julian D.G., Camm A.J., Frangin G., Janse M.J., Munoz A., Schwartz P.J., Simon P. (1997) Randomised trial of effect of amiodarone on mortality

in patients with left-ventricular dysfunction after recent myocardial infarction: EMIAT. European Myocardial Infarct Amiodarone Trial Investigators. *Lancet* 349, 667-674.

2. Li M., Zheng C., Sato T., Kawada T., Sugimachi M., Sunagawa K. (2004) Vagal nerve stimulation markedly improves long-term survival after chronic heart failure in rats. *Circulation* 109, 120-124.

3. Krieg T., Qin Q., Philipp S., Alexeyev M.F., Cohen M.V., Downey J.M. (2004) Acetylcholine and bradykinin trigger preconditioning in the heart through pathway that includes Akt and NOS. *Am. J. Physiol. Heart Circ. Physiol.* 287, H2606-H2611.

4. Semenza G.L. (2003) HIF-1, O(2), and the 3 PHDs: how animal cells signal hypoxia to the nucleus. *Cell* 107, 1-3.

5. Kakinuma Y., Miyauchi T., Yuki K., Murakoshi N., Goto K., Yamaguchi I. (2001) Novel molecular mechanism of increased myocardial endothelin-1 expression in the failing heart involving the transcriptional factor hypoxia-inducible factor-1a induced for impaired myocardial energy metabolism. *Circulation* 103, 2387-2394.

6. Maxwell P.H., Wiesener M.S., Chang G.W., Clifford S.C., Vaux E.C., Cockman M.E., Wykoff C.C., Pugh C.W., Maher E.R., Ratcliffe P.J. (1999) The tumour suppressor protein VHL targets hypoxia-inducible factors for oxygen-dependent proteolysis. *Nature* 399, 271-275.

7. Min J.H., Yang H., Ivan M., Gertler F., Kaelin W.G. Jr., Pavletich N.P. (2002) Structure of an HIF-1alpha -pVHL complex: hydroxyproline recognition in signaling. *Science* 296, 1886-1889.

8. Page E.L., Robitaille G.A., Pouyssegur J., Richard D.E. (2002) Induction of hypoxia-inducible factor-1alpha by transcriptional and translational mechanisms. *J. Biol. Chem.* 277, 48403-48409.

9. Richard D.E., Berra E., Pouyssegur J. (2000) Nonhypoxic pathway mediates the induction of hypoxia-inducible factor 1alpha in vascular smooth muscle cells. *J. Biol. Chem.* 275, 26765-26771.

10. Zanella B., Calonghi N., Pagnotta E., Masotti L., Guarnieri C. (2002) Mitochondrial nitric oxide localization in H9c2 cells revealed by confocal microscopy. *Biochem. Biophys. Res. Commun.* 290, 1010-1014.

11. Okudela K., Hayashi H., Ito T., Yazawa T., Suzuki T., Nakane Y., Sato H., Ishi H., KeQin X., Masuda A., Takahashi T., Kitamura H. (2004) K-ras gene mutation enhances motility of immortalized airway cells and lung adenocarcinoma cells via Akt activation: possible contribution to non-invasive expansion of lung adenocarcinoma. *Am. J. Pathol.* 164, 91-100.

12. Chen J., Zhao S., Nakada K., Kuge Y., Tamaki N., Okada F., Wang J., Shindo M., Higashino F., Takeda K., Asaka M., Katoh H., Sugiyama T., Hosokawa M., Kobayashi M. (2004) Dominant-negative hypoxia-inducible factor-1 alpha reduces tumorigenicity of pancreatic cancer cells through the suppression of glucose metabolism. *Am. J. Pathol.* 162, 1283-1291.

13. Du X.J., Dart A.M., Riemersma R.A., Oliver M.F. (1990) Failure of the cholinergic modulation of norepinephrine release during acute myocardial ischemia in the rat. *Circ. Res.* 66, 950-956.

14. Kim C.H., Cho Y.S., Chun Y.S., Park J.W., Kim M.S. (2002) Early expression of myocardial HIF-1alpha in

response to mechanical stresses: regulation by stretch-activated channels and the phosphatidylinositol 3-kinase signaling pathway. *Circ. Res.* 90, e25-e33.

15. Sandau K.B., Zhou J., Kietzmann T., Brune B. (2001) Regulation of the hypoxia-inducible factor 1alpha by the inflammatory mediators nitric oxide and tumor necrosis factor-alpha in contrast to desferroxamine and phenylarsine oxide. *J. Biol. Chem.* 276, 39805-39811.

16. Vanhaesebroeck B., Alessi D.R. (1999) The regulation and activities of the multifunctional serine/threonine kinase Akt/PKB. *Exp. Cell Res.* 253, 210-229.

17. Kennedy S.G., Wagner A.J., Conzen S.D., Jordan J., Bellacosa A., Tsichlis P.N., Hay N. (1997) The PI3-kinase/Akt signaling pathway delivers an anti-apoptotic signal. *Genes Dev.* 11, 701-713.

18. Cross D.A., Alessi D.R., Cohen P., Andjelkovich M., Hemmings B.A. (1995) Inhibition of glycogen synthase kinase-3 by insulin mediated by protein kinase B. *Nature* 378, 785-789.

19. Zhou J., Schmid T., Brune B. (2003) Tumor necrosis factor-alpha causes accumulation of a ubiquitinated form of hypoxia inducible factor-1alpha through a nuclear factor-kappaB-dependent pathway. *Mol. Biol. Cell* 14, 2216-2225.

20. Sandau K.B., Fandrey J., Brune B. (2001) Accumulation of HIF-1alpha under the influence of nitric oxide. *Blood* 97, 1009-1015.

21. Metzen E., Zhou J., Jelkmann W., Fandrey J., Brune B. (2003) Nitric oxide impairs normoxic degradation of HIF-1alpha by inhibition of prolyl hydroxylases. *Mol. Biol. Cell* 14, 3470-3481.

22. Xi L., Taher M., Yin C., Salloum F., Kukreja R.C. (2004) Cobalt chloride induces delayed cardiac preconditioning in mice through selective activation of HIF-1{alpha} / AP-1 and iNOS Signaling. *Am. J. Physiol. Heart. Circ. Physiol.* 287, H2369-H2375.

23. Hirota K., Fukuda R., Takabuchi S., Kizaka-Kondoh S., Adachi T., Fukuda K., Semenza G.L. (2004) Induction of hypoxia-inducible factor 1 activity by muscarinic acetylcholine receptor signaling. *J. Biol. Chem.* 279, 41521-41528.

24. Wang H., Yu M., Ochani M., Amella C.A., Tanovic M., Susarla S., Li J.H., Wang H., Yang H., Ulloa L., Al-Abed Y., Czura C.J., Tracey K.J. (2003) Nicotinic acetylcholine receptor alpha7 subunit is an essential regulator of inflammation. *Nature* 421, 384-388.

Figure legends

Figure 1

HIF-1a is induced by ACh in rat cardiomyocytes even under normoxia.

A. After treatment of H9c2 cells with 1 mM ACh for 8 hours, the HIF-1a protein level is increased (# p<0.05 vs. control, n=4). B. ACh (1 mM) increases the intensity of DAF-2DA fluorescence (# p<0.01 vs. control, n=3).

Figure 2

HIF-1α induction by ACh is posttranslationally regulated in rat cardiomyocytes under normoxia.

A. The HIF-1α protein level in H9c2 cells in the presence of 0.5 μg/ml of actinomycin D is increased by 1 mM ACh to a comparable level to

that in the absence of actinomycin D (N.S., not significant, n=3). **B.** Actinomycin D does not decrease the HIF-1α mRNA level, as evaluated by RT-PCR. **C.** Cycloheximide (10 µg/ml) does not affect the HIF-1α protein level (n=3).

Figure 3
Rat primary cultured cardiomyocytes show comparable HIF-1α induction by 1 mM ACh to that in H9c2 cells (# p<0.05 vs. control, n=3).

Figure 4
Akt is activated by ACh in rat cardiomyocytes, leading to HIF-1α induction.
A. Akt phosphorylation in H9c2 cells is rapidly increased by 1 mM ACh (# p<0.05 vs. baseline, n=4), whereas the total protein level of Akt remains unaffected. **B.** The ACh-induced increase in Akt phosphorylation is blocked by 1 mM atropine (# p<0.05 vs. 0 µM atropine, n=3). **C.** ACh (1 mM) also increases Akt phosphorylation in rat primary cardiomyocytes (# p<0.05 vs. baseline, n=3), and atropine blocks this effect. **D.** Pretreatment with 300 nM wortmannin completely inhibits ACh-induced Akt phosphorylation in H9c2 cells (N.S., not significant, n=3). **E.** Wortmannin (300 nM) also inhibits HIF-1α induction by ACh (# p<0.05 vs. wortmannin (+), n=3). Each figure shows a representative result from 3 independently performed experiments (n=3). **F.** In contrast to wt Akt, HIF-1α induction y ACh is blocked by dn Akt in HEK293 cells (n=4).

Figure 5
Collapse of the mitochondrial membrane potential in rat cardiomyocytes under hypoxia is attenuated by ACh pretreatment.
A. Hypoxia decreases the mitochondrial membrane potential in H9c2 cells within 12 hours. Red spots are decreased by hypoxia, whereas pretreatment with 1 mM ACh for 12 hours inhibits this effect. **B.** Pretreatment with 1 mM ACh inhibits the decrease in MTT reduction activity induced by 12 hours of hypoxia not only in H9c2 cells (# p<0.01 vs. hypoxia, n=8) but also in HEK293 cells (* p<0.01 vs. hypoxia, n=8). **C.** Hypoxia increases caspase-3 activity, whereas pretreatment with 1 mM ACh inhibits this effect (# p<0.01 vs. hypoxia, n=3). **D.** In contrast to wt HIF-1α or GFP, dn HIF-1α alone decreases the MTT activity under hypoxia after ACh treatment (# p<0.01 vs. wt and GFP, * p<0.05 vs. non-transfection, n=10).

Figure 6
Vagal nerve stimulation decreases infarcted area with increased HIF-1a expression.
A. A quantitative analysis reveals comparable non-perfused areas in both vagal-stimulated (MI-VS) and non-stimulated (MI) hearts, whereas the infarcted area identified by TTC staining is smaller in the MI-VS heart than in the MI heart. **B.** HIF-1α induction in the ischemic heart is increased by vagal stimulation (MI-VS) compared with that in ischemia alone (MI) (#, p<0.01 vs. MI) (n=3).

Figure 7
HIF-1a is induced by ACh under normoxia in other cells.
ACh (1 mM) increases HIF-1a protein level in HEK293 and HeLa cells (n=3 each) under normoxia.
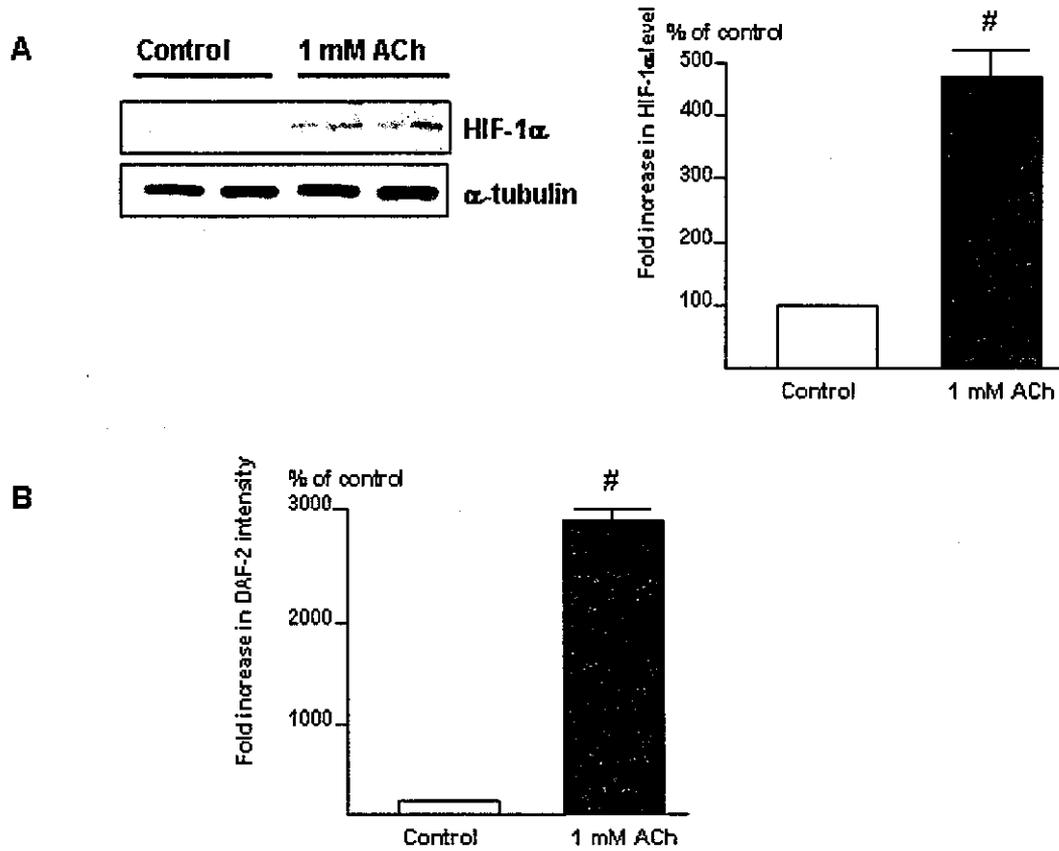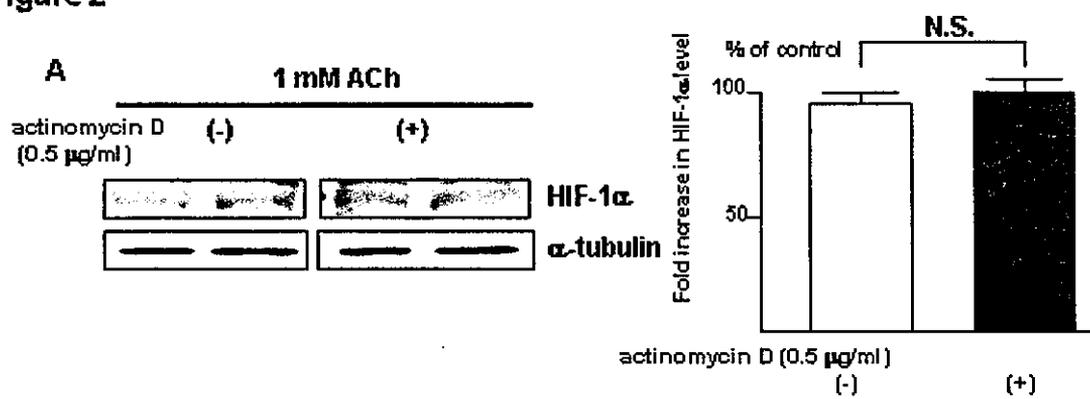
Kakinuma Y et al
Figure 1
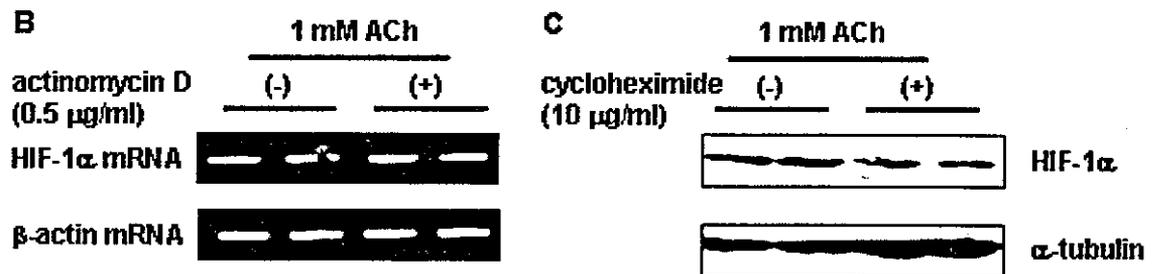
A

B

Figure 2

A

Kakinuma Y et al
Figure 2

B | 1 mM ACh

B

1 mM ACh

actinomycin D   (-)   (+)
(0.5 µg/ml)

HIF-1α mRNA

β-actin mRNA

C

1 mM ACh

cycloheximide   (-)   (+)
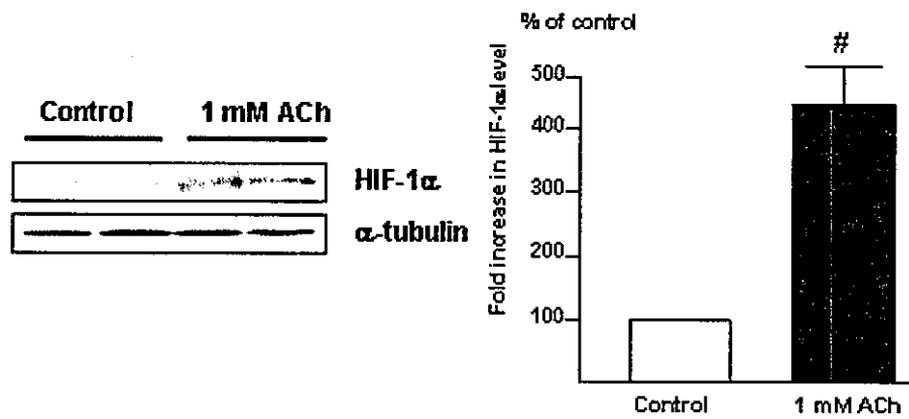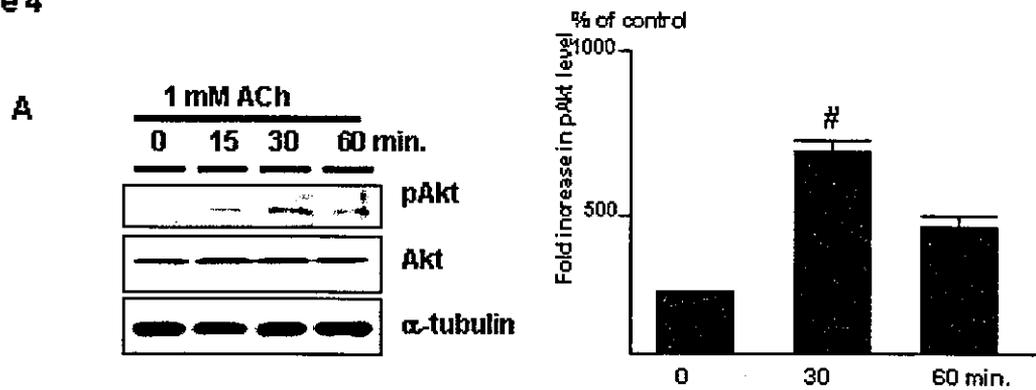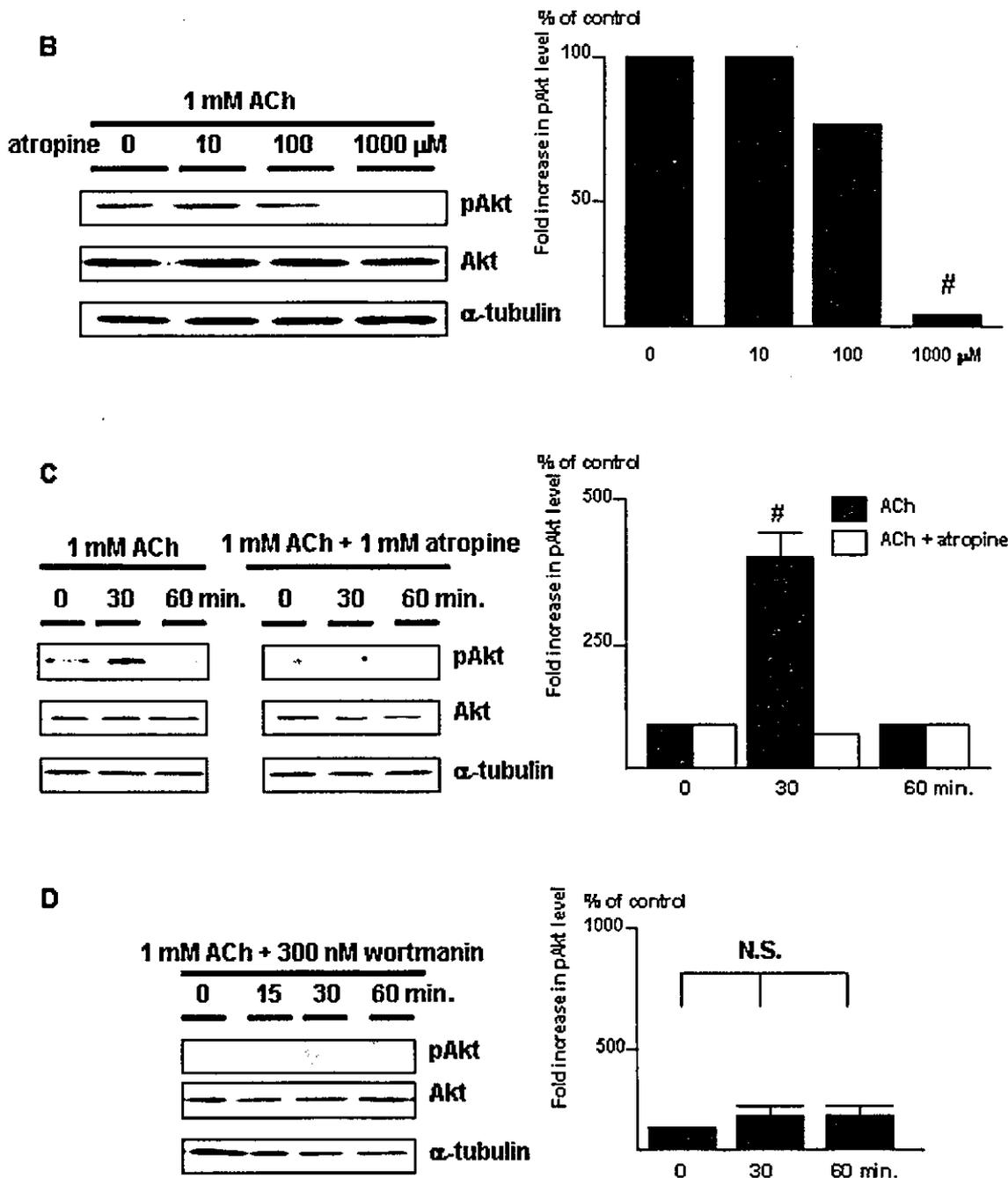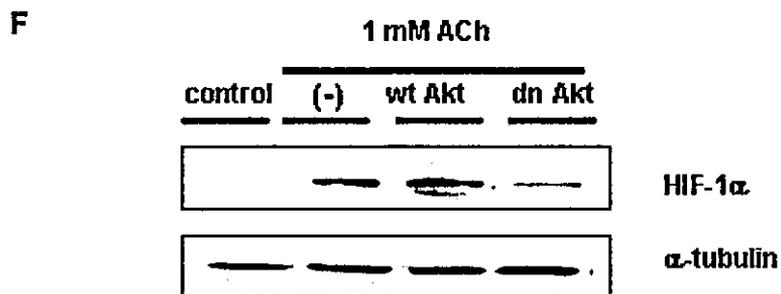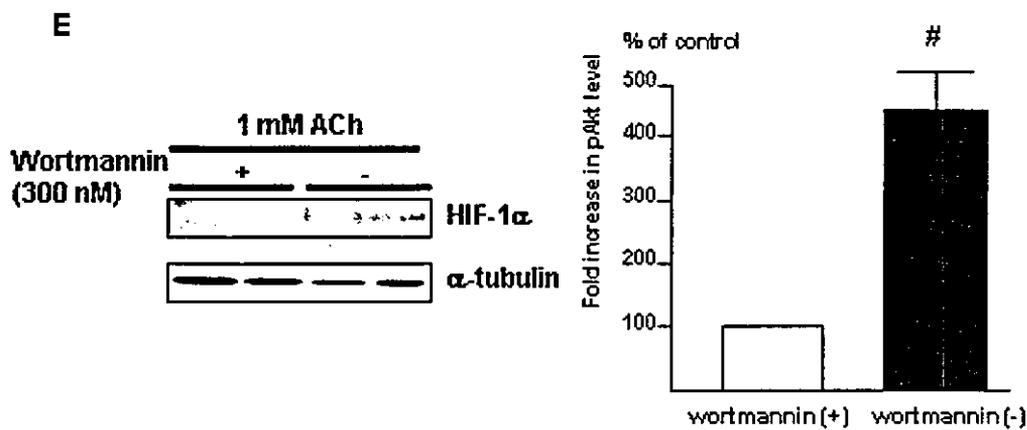(10 µg/ml)

HIF-1α

α-tubulin

Figure 3

Figure 4

A

Kakinuma Y et al
Figure 4

Kakinuma Y et al
Figure 4

E

1 mM ACh

Wortmannin
(300 nM)   +   -

HIF-1α

α-tubulin

% of control

Fold increase in pAkt level

500
400
300
200
100

#

wortmannin (+)   wortmannin (-)

F

1 mM ACh

control   (-)   wt Akt   dn Akt

HIF-1α

α-tubulin

Figure 5

A

control   hypoxia   1 mM ACh + hypoxia

Kakinuma Y et al
Figure 5

B

H9c2 cells

Fold increase in MTT activity

% of control

100 —

50 —

control   hypoxia   ACh + hypoxia

\#

HEK293 cells

Fold increase in MTT activity

% of control

100 —

50 —

control   hypoxia   ACh + hypoxia

*

C

Fold increase in caspase-3 activity

200% —

100% —

H9c2 cells

□ control
■ 1 mM ACh

0 hr   12 hrs

\#

D

Fold increase in MTT activity

% of control

1 mM ACh + hypoxia

100 —

50 —

non-transfection   wt HIF-1α   dn HIF-1 α   GFP

\#
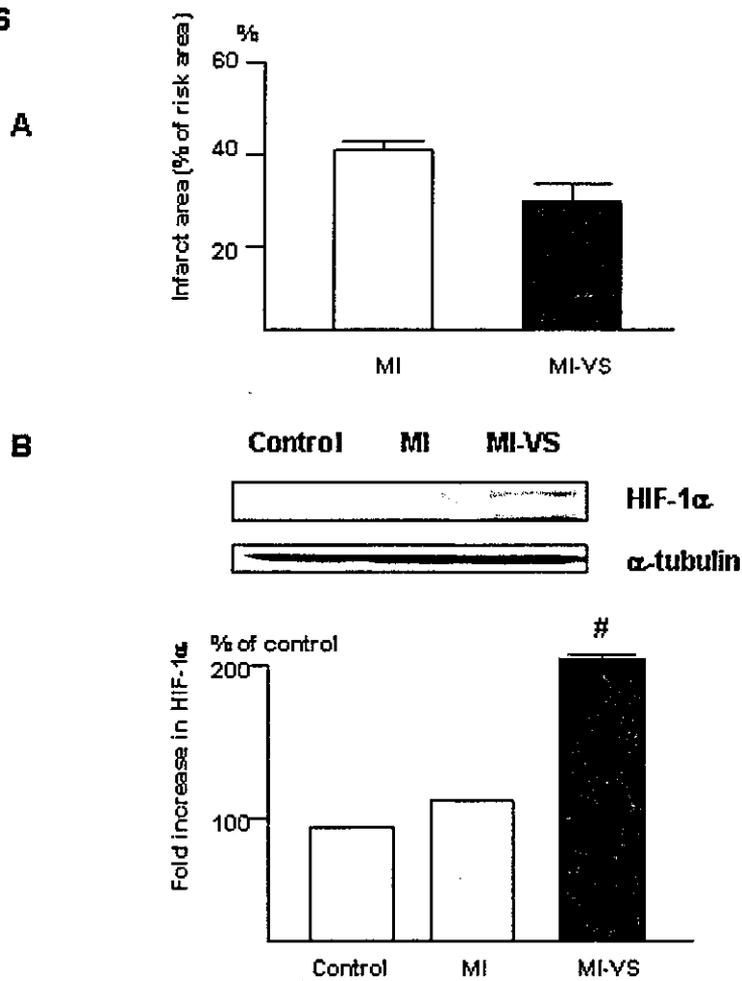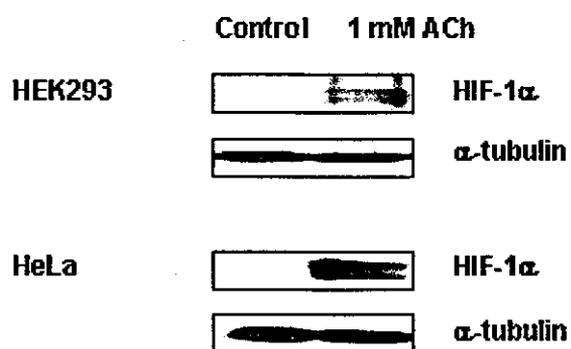*

Kakinuma Y et al
Figure 6

A

B

Figure 7

HIF-1α is Involved in the Attenuation of Experimentally Induced Rat Glomerulonephritis

Yoshihiro Kudo[1], Yoshihiko Kakinuma[2], Yasukiyo Mori[3], Norihito Morimoto[1], Takashi Karashima[4], Mutsuo Furihata[5], Takayuki Sato[2], Taro Shuin[4], Tetsuro Sugiura[1]

Departments of [1]Laboratory Medicine, [2]Cardiovascular Control, [4]Urology and [5]Tumor Pathology, Kochi Medical School, Kochi, Japan
[3]The Second Department of Internal Medicine, Kansai Medical University, Osaka, Japan

Address for Correspondence; Yoshihiko Kakinuma, M.D., Ph.D. Department of Cardiovascular Control, Kochi Medical School, Kochi 783-8505, Japan
Phone: +81-88-880-2311, Fax: +81-88-880-2310, E-mail: kakinuma@med.kochi-u.ac.jp

Abstract

Background/Aim: Among various kidney disease models, there are few rat glomerulonephritis (GN) models that develop in a short time, and with mainly glomerular lesions. Hypoxia-inducible factor (HIF)-1α is a transcriptional factor that induces genes supporting cell survival, but the involvement of HIF-1α in attenuating the progression of GN remains to be elucidated. We developed a new model of rat GN by co-administration of Angiotensin II (AII) with Habu snake venom (HV) and investigated whether HIF-1α is involved in renal protection. *Methods:* Male Wistar rats were unilaterally nephrectomized on day −1, and divided into 4 groups on day 0; N group (no treatment), HV group, A group (AII), and H+A group (HV and AII). To pre-induce HIF-1α, cobalt chloride ($CoCl_2$) was injected twice before injections of HV and AII in 11 rats.
Results: GN was detected only in the H+A group; observed first on day 2 and aggravated thereafter. HIF-1α was expressed in the glomeruli and renal tubules in the A and H+A groups. In the H+A group, GN was remarkably reduced by $CoCl_2$ pre-treatment (44.9% to 12.2%, $p<0.01$). *Conclusion:* Both HV and AII were critical for the development of GN, and HIF-1α remarkably attenuated the progression of GN.

Key Words

Glomerulonephritis, Habu snake venom, Angiotensin II, HIF-1α

Introduction

Many animal studies have been performed in attempts to overcome the poor prognosis of chronic renal failure due to diabetic nephropathy and glomerulonephritis (GN) [1-5]. Although factors involved in the pathogenesis of GN have been intensively investigated, the development of a proper animal GN model with high reproducibility and simplicity as well as a model without time-consuming process are required. Experimental rat models of GN are classified into several groups in terms of the pathophysiological mechanisms of renal diseases. Anti-glomerular basement membrane (GBM) nephritis was developed with depositions of immune complex using anti-glomerular basement membrane antibody [3,6], tubulo-interstitial injury was caused by cyclosporine A [4] and injury of renal tubules by ischemia [5]. However, there are few rat GN models with mainly pathological features in the glomeruli that are developed in a short time [7]. Angiotensin II (AII) is known to increase blood pressure through vascular contraction, and to be profoundly involved in vascular hypertrophy and the contraction of intrarenal arteries. AII is also directly involved in the progression of glomerulosclerosis via the effect of hyperfiltration with or without hypertension [8,9]. Many studies have revealed important factors involved in the pathogenesis of GN or factors aggravating GN, but evaluating further factors that suppress the occurrence of GN is also crucial. To investigate the features of renal protection, we focused on hypoxia-inducible factor (HIF)-1α. HIF-1α, a transcriptional factor with formation of a heterodimer with HIF-1β [10], is post-transcriptionally regulated and its protein level is elevated by hypoxia through inhibition of ubiquitin-mediated degradation. HIF-1α is known to be a survival factor responsible for inducing lines of genes supporting cell survival such as glucose metabolism (glucose transporters and glycolysis enzymes), vasomotor regulation (heme oxygenase-1 and endothelin-1), angiogenic growth (vascular endothelial growth factor), and anemia control (erythropoietin and transferrin) [11-13]. Recent studies have demonstrated that non-hypoxic stimuli like AII can also activate HIF-1α [14,15], but the role of HIF-1α induction in attenuating the progression of GN remains to be elucidated. Accordingly, we

developed a new rat GN model by co-administration of AII with Habu snake venom (HV) and investigated whether pre-induction of HIF-1α leads to renal protection.

Materials and Methods
Development of Rat GN Model

All experiments were approved by the institutional review board for the care of animal subjects and were performed in accordance with guidelines of Kochi Medical School. Nine-weeks old male Wistar rats (180-220g) were purchased from Japan SLC (Shizuoka, Japan). Rats were unilaterally nephrectomized on day -1. On day 0, the rats were divided into 4 groups. In the first group, no treatment was performed with any reagents or surgical procedure (N group, n=6). In the second group, rats were injected with 3.5 mg/kg of HV (Sigma-Aldrich Co., Steinheim, Germany) through the femoral vein (HV group, n=11). In the third group, rats were continuously administered with AII (100ng/min, Peptide Institute, Inc., Osaka, Japan) using Alzet osmotic pumps (DURECT Co., Cupertino, CA) (A group, n=11). In the fourth group, rats were administered with both HV and AII (H+A group, n=22). Rats were sacrificed on days 1, 2, 3 or 4, and kidneys excised for histochemical analysis (fig. 1).

Measurement of Systolic Blood Pressure

Systolic blood pressure (SBP) was measured by the tail-cuff method with an electro-sphygmomanometer (BP-98A, Softron Co., Tokyo, Japan). SBP was measured in conscious rats every day from day -1 to day 2. The SBP value for each rat was calculated as the average of 3 separate measurements at each session. SBP measurement was performed between 9 and 12 a.m. by a single blinded investigator.

Measurements of Serum Urea Nitrogen and Creatinine

Before the sacrifice, blood samples were obtained via an axillary vein for determination of serum urea nitrogen (UN) and creatinine (Cr) levels. Serum UN and Cr levels were determined enzymatically with automation-analysis equipment (Hitachi 7350, Hitachi Co., Ibaragi, Japan) in our laboratory center.

Histological Analysis

To evaluate the progression of GN in our animal model, histological analyses were performed using the periodic acid-Schiff (PAS) and periodic acid-methenamine silver (PAM) reagents. After the specimens were paraffin-embedded, 4-micrometer sectioned samples were stained with PAS and PAM reagents and counterstained with hematoxylin. For quantitative analysis, the ratio of damaged glomeruli to all glomeruli in the sectioned sample was calculated and the percentage of GN in the section was evaluated. Moreover, semiquantitative analysis

was performed to evaluate more precisely the morphological changes of our GN model according to the protocol in previous studies [16,17]. A minimum of 20 glomeruli (ranging from 20 to 60 glomeruli) in each specimen were examined and the severity of the mesangiolysis lesion was graded from 0 to 4+ according to the percentage of glomerular involvement; a 1+ lesion represented an involvement of 25 % of the glomerulus while a 4+ lesion indicated that 100 % of the glomerulus was involved. Thus, the mesangiolysis score (MES) was then obtained by multiplying the degree of damage (0 to 4+) by the percentage of the glomeruli with the lesion. Tubular injuries including tubular necrosis or occlusion of collecting ducts by cast material were graded as mild (1+), moderate (2+), or severe (3+).

Western Blot Analysis

Nuclear protein from whole kidney was prepared using NE-PER Nuclear and Cytoplasmic Extraction Reagents (Pierce Biotechnology, Inc. Rockford, Illinois, USA). Nuclear protein was electrophoresed using 10% SDS-PAGE gels and transferred to polyvinylidene difluoride membrane (Immobilon-P, Millipore Co., Bedford, Massachusetts, USA). A monoclonal IgG HIF-1α antibody α67 (Novus Biological, Littleton, Colorado, USA) was used; a horseradish peroxidase-conjugated antibody (Promega Co., Madison, USA) was used as a secondary antibody. The ECL Western blotting systems (Amersham Bioscience, Upsala, Sweden) was used for detection.

Immunohistochemical Analysis

Paraffin sections including the samples were dewaxed in xylene and rehydrated in a series of ethanol, and then washed in distilled water before staining procedures. According to the instruction provided by the manufacturer, HIF-1α was identified with rabbit polyclonal anti-HIF-1α antibody H-206 (Santa Cruz Biotechnology, California, USA) utilizing the catalyzed signal amplification system (Dako, Hamburg, Germany) based on the streptavidin-biotin-peroxidase reaction. Antigen retrieval was performed for 5 min in a preheated Dako target retrieval solution using a microwave. Incubation procedures were performed in a humidified chamber. Following the incubation, specimens were washed 3 times in TBST buffer. The specificity of staining was confirmed by substitution of the primary antibody for a normal rabbit IgG and additionally by an immunohistochemical reaction without a primary antibody but with the secondary antibody alone.

An Experiment using Cobalt Chloride as a Pretreatment

Rats were twice subcutaneously administered 30mg/kg of cobalt chloride ($CoCl_2$) at a 12 hour interval ($CoCl_2$ group) (n=11), followed by unilateral

nephrectomy. Then, the rats were administered with HV and AII. As a comparison, rats were injected with 0.9% NaCl solution instead of $CoCl_2$, followed by the same protocol as the $CoCl_2$ group (n=11). After $CoCl_2$ administration, however, before injection of HV and AII, a kidney was excised as a sample to examine expression level of HIF-1α ($CoCl_2$ Pre). Likewise, 2 days after administration of HV and AII, a kidney was also excised ($CoCl_2$ Day2). To compare the expression level of HIF-1α by $CoCl_2$ before GN and the severity of pathology of GN, we investigated whether pre-induction of HIF-1α. is involved in renal protection.

Statistical Analysis

Data are reported as mean ± SEM. A paired *t* test was used for paired samples and Student's *t* test was used to compare the 2 groups. One-way layout analysis of variance or repeated measures of analysis of variance were used to compare multiple groups. If the p value was significant, Scheffe's multiple comparison was performed. A p value < 0.05 were considered significant.

Results

AII combined with HV developed GN

Morphological studies using PAS and PAM staining revealed that there are no glomerular or tubular injuries in N group (fig. 2A), HV group (fig. 2B), A group (fig. 2C), however, GN was detected only in the H+A group (fig. 2E). Although renal tubular casts were observed, glomerular changes were scarcely observed on day 1 after AII and HV administration (figs. 2D, 3). GN was initially detected on day 2 (figs. 2E, 2F, 3), followed by further aggravation during the time course (data not shown). Renal tubular injury including tubular necrosis was not remarkable, and extensive cellular infiltration was not found in the interstitial regions (fig. 3). On the other hand, characteristic focal and segmental mesangiolysis, explained as capillary aneurysmal ballooning, was observed with dilatation of glomerulus (figs. 2E, 2F). The rate of occurrence of GN on day 2 was 44.9±2.6 %, and the MES score of the H+A group was 199±15 (fig. 3). On the other hand, in the HV group, less than 2 % had morphologic changes of mesangiolysis during 4 days, and the MES score was 10±5 (figs. 2B, 3). Moreover, in the A group, there were no morphologic changes during the time course (fig. 2C).

Changes in serum UN and Cr

Serum UN and Cr were 18.4±0.7, 0.31±0.01 mg/dl, respectively, on day 2 in the N group. In the H+A group, serum UN and Cr levels increased to 41.5±4.0, 0.57±0.05 mg/dl, respectively, on day 2; significantly higher than those in the N group (figs. 4A, 4B). In contrast, serum UN and Cr levels in the H+A group on day 1 (24.0±1.8 and 0.42±0.02 mg/dl, respectively) were similar to the level of the N group.

There were no significant differences in serum UN and Cr level among the HV, A and N groups.

SBP response

SBP values of each group are shown in figure 4C. There were no significant differences in SBP after nephrectomy among the 4 groups. Administration of AII caused a significant increase of SBP on day 1 (186±4 mmHg) and persisted to day 2 (192±1 mmHg). SBP in the H+A group on day 2 (183±3 mmHg) was comparable to that in the A group. Administration of HV had no influence on SBP during the 2 days.

Expression Level of HIF-1α Protein

Western blot analysis revealed that the expression level of HIF-1α protein increased in the H+A and A groups (fig. 5A), compatible with the results of immunohistochemical analysis. Expressions of HIF-1α protein were observed in the A and H+A groups, but protein expression was not detected in the N and HV groups. These data suggest that HIF-1α was induced mainly by AII, and, at least in part, was related to the pathogenesis of GN or to the defense mechanism against the progression of GN.

Induction of HIF-1α in Glomeruli and Renal Tubules

Immunohistochemical study demonstrated positive nuclear staining of HIF-1α in glomeruli, renal tubules (figs. 2I, 2J), collecting ducts and epithelium of the papilla (data not shown) in the A and H+A groups. In contrast, no positive nuclear signals were detected in the N (fig. 2H) and HV (data not shown) groups. HIF-1α positive cells were mainly detected in mesangial cells in glomeruli (figs. 2I, 2J). As demonstrated, especially in the H+A group (fig. 2J), HIF-1α was expressed in the intact part of the glomerulus, but not in the injured part of the same glomerulus. Furthermore, nuclear HIF-1α positive signals were observed in smooth muscle cells in peripheral renal arteries (data not shown).

CoCl_2 Pretreatment Inhibits the Progression of GN

To further investigate whether HIF-1α is involved in the development of nephropathy or in the anti-progressive action, we pretreated rats with $CoCl_2$. As demonstrated in fig. 5B, pretreatment with $CoCl_2$ increased HIF-1α expression before administration of HV and AII (Pre-1), suggesting that HIF-1α was induced by $CoCl_2$ before development of GN. Even on day 2, the expression level of HIF-1α was increased in the $CoCl_2$ group ($CoCl_2$ Day2-1). In the $CoCl_2$ group, focal mesangiolysis with glomeruli enlargement was still observed, but the number of GN was much less than in those without $CoCl_2$ pretreatment (fig. 2G).

Thus, 7 of 11 rats (63.6%) with $CoCl_2$ pretreatment were rescued from GN alone, while the other 4 (36.4%) were not; showing a comparable severity level of GN with the non-$CoCl_2$ group. As

demonstrated in fig. 5B, unlike Pre-1, Pre-2 did not induce HIF-1α with $CoCl_2$ and showed no $CoCl_2$ suppression of GN. The ratio between rats rescued or not-rescued from GN was comparable with that between pre-induction and non-induction of HIF-1α by $CoCl_2$, as demonstrated in fig. 5C. In the $CoCl_2$ group the rate of GN from each rat decreased to 12.2±2.1%, which was in great contrast to 44.9±2.6% in the non-$CoCl_2$ group. Furthermore, serum UN and Cr levels on day 2 were significantly lower in the $CoCl_2$ than in the non-$CoCl_2$ group ($p<0.05$) (figs. 6A, 6B), despite comparable SBP values between the 2 groups (fig. 6C).

Discussion

In this study, we developed a new model of GN induced by both HV and AII. This model has several distinct characteristics. First, GN developed rapidly, and was detected on the second day after administration of HV and AII. Many models of GN have been reported including 5/6 nephrectomized and Thy-1.1 nephritis models [18,19]. However, these models take a long time to develop nephropathy. In contrast, our protocol induced GN in 2 days, suggesting that one of the advantages our model has over others is in terms of the time course. Further, pathological findings were restricted to glomerular regions without remarkable tubular or interstitial lesions. Since our GN model developed within 2 days, our model also has advantages for disclosing the specifically critical time point of the development of GN. Further, the development rate of GN was almost 100%, indicating the high reproducibility of our model. This basis of the rat model was initially developed by Barnes JL et al. who reported that the progression of AII-induced renal injury was accelerated by preexisting injury induced by HV [20]; ours, which now optimizes the reproducibility of GN, is a modification of their model.

Habu induced nephropathy was reported to develop within 1 day by a dose of 2.0-4.0 mg/kg HV (in our model 3.5 mg/kg) and the main pathological change was "mesangiolysis" [21,22]. However, for reasons we haven't as yet ascertained, in our study no rats showed Habu-nephropathy specific pathological findings during the first week in the HV group. On the other hand, AII is one of the major factors responsible for the pathogenesis of GN, because it remarkably increases glomerular pressure causing hyperfiltration, production of extracellular matrix and expression of lines of genes involving GN [23-25]. Further, since AII has some ischemic effects on kidney, there is the possibility that an AII-induced ischemic effect causes the GN depicted in our model. However, as demonstrated in this study, glomerular injury was predominantly observed, and was not associated with renal tubular lesions, i.e., tubular necrosis suggesting renal ischemia. Therefore, in accordance with the pathological characteristic of this

GN, AII-induced renal ischemia may not be responsible for the development in our model. Additionally, in this study, SBP increased in the A and A+H groups, but GN was not induced in the A group. Therefore, GN in our model was induced not by HV or AII alone, but by the combination of HV and AII, independent of any increase in systemic blood pressure.

HIF-1α is a master transcriptional factor, transactivating the expression of many genes important for cell survival under hypoxic conditions [11-13,26]. These genes are responsible for glycolysis, angiogenesis, proliferation and iron metabolism, all of which are induced by hypoxic stress; thus, the induction of HIF-1α is a marker of hypoxia. HIF-1α is regulated at the post-translational level by the proteasome system through ubiquitination with von Hippel Lindeau (VHL) protein [27,28]. As previously reported, this regulation of HIF-1α protein level is dependent on the concentration of oxygen. Hypoxia induces enhancement of HIF-1α protein stability leading to the elevation of the protein level due to inhibition of degradation by VHL. Therefore, hypoxia induces adaptation in cells including induction of HIF-1α; the hypoxic pathway. On the other hand, a line of evidence has recently accumulated that suggests that HIF-1α is also regulated independent of oxygen concentration through the non-hypoxic pathway [14,15]. AII is reported to regulate HIF-1α both at transcriptional and post-translational levels in vascular smooth muscle cells cultured under normoxic condition through the AII type 1 receptor [14,15]. Moreover, HIF-1α is also post-translationally regulated in several cell lines in the presence of tumor necrosis factor-α or nitric oxide independent of oxygen contents [29,30].

As demonstrated in this study, immunoreactivity of HIF-1α was not detected in the N group (no treatment group), but HIF-1α was detected in the nuclei of glomerular, tubular and epithelium cells of the papilla by administration of AII alone or AII and HV together. This is the first evidence showing that HIF-1α was detected in the kidney by AII, independent of systemic hypoxic stress. As indicated here, HIF-1α was found to be expressed only in intact, not damaged glomeruli. Even within a glomerulus, only the intact part of glomerular cells expressed HIF-1α. Considering the fact that induction of HIF-1α is one of the defense mechanisms for cell survival [31-33], our data indicate that induction of HIF-1α is a marker of glomeruli survival; indeed, it could be a marker of renal protection.

To further investigate whether HIF-1α is involved in the progression or protection of GN, pre-induction of HIF-1α was performed with $CoCl_2$ before administration of HV and AII. Surprisingly, the induction of HIF-1α by $CoCl_2$ pretreatment

attenuated the progression of GN; the level of GN was reduced from 44.9% to 12.2% and the incidence of GN was reduced from 100% to 36.4%. Furthermore, as indicated, the pre-induction of HIF-1α actually affects the inhibition of GN, because the rate of HIF-1α induction was parallel with that of the attenuation of GN. Therefore, our data suggest that HIF-1α is involved, at least in part, in the defense mechanism against the progression of GN, and hence could be a marker for renal protection.

AII is reported to induce HIF-1α [14,15] and it plays a partial role in the renal protective effect; however, the other effects of AII, such as increasing glomerular pressure and modulating gene expression involving in the renal failure, may overcome any protective effect of AII-induced HIF-1α, and so as a result it may lead to the progression of GN.

In conclusion, we developed a highly reproducible GN model by combining HV and AII. Pre-induction of HIF-1α remarkably attenuated the progression of GN, indicating that HIF-1α was involved in the defense mechanism of the kidney.

References

1 Rifai A, Small PA Jr, Teague PO, Ayoub EM: Experimental IgA nephropathy. J Exp Med 1979; 150: 1161-1173.

2 Ishizaki M, Masuda Y, Fukuda Y, Yamanaka N, Masugi Y, Shichinohe K, Nakama K: Renal lesions in a strain of spontaneously diabetic WBN/Kob rats. Acta Diabetol Lat 1987; 24: 27-35.

3 Banks KL: Glomerulonephritis, autoimmunity, autoantibody. Animal model: anti-glomerular basement membrane antibody in horses. Am J Pathol 1979; 94: 443-446.

4 Elzinga LW, Rosen S, Bennett WM: Dissociation of glomerular filtration rate from tubulointerstitial fibrosis in experimental chronic cyclosporine nephropathy: role of sodium intake. J Am Soc Nephrol 1993; 4: 214-221.

5 Arendshorst WJ, Finn WF, Gottschalk CW: Pathogenesis of acute renal failure following temporary renal ischemia in the rat. Circ Res 1975; 37: 558-568.

6 Wilson CB, Dixon FJ: Immunopathologic mechanisms of renal disease. Ric Clin Lab 1975; 5: 17-38.

7 Masuda Y, Shimizu A, Mori T, Ishiwata T, Kitamura H, Ohashi R, Ishizaki M, Asano G, Sugisaki Y, Yamanaka N: Vascular endothelial growth factor enhances glomerular capillary repair and accelerates resolution of experimentally induced glomerulonephritis. Am J Pathol 2001; 159: 599-608.

8 Kim S, Iwao H: Molecular and cellular mechanisms of angiotensin II-mediated cardiovascular and renal diseases. Pharmacol Rev 2000; 52: 11-34.

9 Lee LK, Meyer TW, Pollock AS, Lovett DH: Endothelial cell injury initiates glomerular sclerosis in the rat remnant kidney. J Clin Invest 1995; 96: 953-964.

10 Huang LE, Arany Z, Livingston DM, Bunn HF: Activation of hypoxia-inducible transcription factor depends primarily upon redox-sensitive stabilization of its alpha subunit. J Biol Chem 1996; 271: 32253-32259.

11 Wang, GL, Jiang BH, Rue EA, and Semenza GL: Hypoxia-inducible factor 1 is a basic-helix-loop-helix-PAS heterodimer regulated by cellular O2 tension. Proc Natl Acad Sci USA 1995; 92: 5510-5514,

12 Rosenberger C, Mandriota S, Jurgensen JS, Wiesener MS, Horstrup JH, Frei U, Ratcliffe PJ, Maxwell PH, Bachmann S, Eckardt KU: Expression of hypoxia-inducible factor-1alpha and -2alpha in hypoxic and ischemic rat kidneys. J Am Soc Nephrol 2002; 13: 1721-1732.

13 Wenger RH, Rolfs A, Marti HH, Guenet JL, and Gassmann M: Nucleotide sequence, chromosomal assignment and mRNA expression of mouse hypoxia-inducible factor-1 alpha. Biochem Biophys Res Commun 1996; 223: 54-59,

14 Richard DE, Berra E, Pouyssegur J: Nonhypoxic pathway mediates the induction of hypoxia-inducible factor 1alpha in vascular smooth muscle cells. J Biol Chem 2000; 275: 26765-26771.

15 Page EL, Robitaille GA, Pouyssegur J, Richard DE: Induction of hypoxia-inducible factor-1alpha by transcriptional and translational mechanisms. J Biol Chem 2002; 277: 48403-48409.

16 Raij L, Azar S, Keane W: Mesangial immune injury, hypertension, and progressive glomerular damage in Dahl rats. Kidney Int 1984; 26: 137-143.

17 Linas SL, Shanley PF, Whittenburg D, Berger E, Repine JE: Neutrophils accentuate ischemia-reperfusion injury in isolated perfused rat kidneys. Am J Physiol 1988; 255: F728-F735.

18 Romero F, Rodriguez-Iturbe B, Parra G, Gonzalez L, Herrera-Acosta J, Tapia E: Mycophenolate mofetil prevents the progressive renal failure induced by 5/6 renal ablation in rats. Kidney Int 1999; 55: 945-955.

19 Kaneko Y, Shiozawa S, Hora K, Nakazawa K: Glomerulosclerosis develops in Thy-1 nephritis under persistent accumulation of macrophages. Pathol Int 2003; 53: 507-517.

20 Barnes JL, Lisa MS: Origin of interstitial fibroblasts in an accelerated model of angiotensin II (AII)-induced interstitial fibrosis. J Am Soc Nephrol 2001; 12: 699A3645.

21 Cattell V, Bradfield JW: Focal mesangial proliferative glomerulonephritis in the rat caused by habu snake venom. A morphologic study. Am J Pathol 1977; 87: 511-524.

22 Kitamura H, Sugisaki Y, Yamanaka N: Endothelial regeneration during the repair process following Habu-snake venom induced glomerular injury. Virchows Arch. 1995; 427: 195-204.

23 Ruggenenti P: Angiotensin-converting enzyme inhibition and angiotensin II antagonism in nondiabetic chronic nephropathies. Semin Nephrol 2004; 24: 158-167.

24 Tolins JP, Raij L: Effects of amino acid infusion on renal hemodynamics. Role of endothelium-derived relaxing factor. Hypertension 1991; 17: 1045-1051.

25 Nakamura T, Obata J, Kimura H, Ohno S, Yoshida Y, Kawachi H, Shimizu F: Blocking angiotensin II ameliorates proteinuria and glomerular lesions in progressive mesangioproliferative glomerulonephritis. Kidney Int 1999; 55: 877-889.

26 Makino Y, Cao R, Svensson K, Bertilsson G, Asman M, Tanaka H, Cao Y, Berkenstam A, Poellinger L: Inhibitory PAS domain protein is a negative regulator of hypoxia-inducible gene expression. Nature 2001; 414: 550-554.

27 Neckers LM: aHIF: the missing link between HIF-1 and VHL? J Natl Cancer Inst 1999; 91: 106-107.

28 Maxwell PH, Wiesener MS, Chang GW, Clifford SC, Vaux EC, Cockman ME, Wykoff CC, Pugh CW, Maher ER, Ratcliffe PJ: The tumour suppressor protein VHL targets hypoxia-inducible factors for oxygen-dependent proteolysis. Nature 1999; 399: 271-275.

29 Zhou J, Fandrey J, Schumann J, Tiegs G, Brune B: NO and TNF-alpha released from activated macrophages stabilize HIF-1alpha in resting tubular LLC-PK1 cells. Am J Physiol Cell Physiol 2003; 284: C439-C446.

30 Sandau KB, Zhou J, Kietzmann T, Brune B: Regulation of the hypoxia-inducible factor 1alpha by the inflammatory mediators nitric oxide and tumor necrosis factor-alpha in contrast to desferroxamine and phenylarsine oxide. J Biol Chem 2001; 276: 39805-39811.

31 Prass K, Ruscher K, Karsch M, Isaev N, Megow D, Priller J, Scharff A, Dirnagl U, Meisel A: Desferrioxamine induces delayed tolerance against cerebral ischemia in vivo and in vitro. J Cereb Blood Flow Metab 2002; 22: 520-525.

32 Furuta GT, Turner JR, Taylor CT, Hershberg RM, Comerford K, Narravula S, Podolsky DK, Colgan SP: Hypoxia-inducible factor 1-dependent induction of intestinal trefoil factor protects barrier function during hypoxia. J Exp Med 2001; 193: 1027-1034.

33 Matsumoto M, Makino Y, Tanaka T, Tanaka H, Ishizaka N, Noiri E, Fujita T, Nangaku M: Induction of renoprotective gene expression by cobalt ameliorates ischemic injury of the kidney in rats. J Am Soc Nephrol 2003; 14: 1825-1832.

Figure Legends

Fig. 1. Study Protocol. All rats are unilaterally nephrectomized on day -1 and divided into 4 groups on day 0.
N group; no injection of reagents. HV group; injection of 3.5mg/kg of Habu snake venom (HV). A group; continuous administration of 100ng/min of Angiotensin II (AII). H+A group; administration of HV and AII.

Fig. 2. Glomerulonephritis is developed with the combination of HV and AII, and HIF-1α is induced in the intact glomeruli.
There are no glomerular or tubular injuries in N group (A), HV group (B), A group (C) and H+A group on day 1 (D). Damaged glomeruli, characterized by extensive mesangiolysis, are observed in H+A group on day 2. PAS staining. Magnification, *100 (E). Focal and segmental mesangiolysis with large capillary aneurysmal ballooning are observed in the H+A group on day 2. PAM staining. Magnification, *400 (F). The number of GN was significantly less in pre-treatment with CoCl₂ than without. PAS staining. Magnification, *100 (G). Immunoreactive HIF-1α positive signals are not detected in the N group (H). Nuclear HIF-1α signals are observed in a glomerulus and tubules in the A group. Magnification, *200 (I). A glomerulus in the H+A group on day 2 possesses intact cells with HIF-1α positive signals, in contrast, other parts have few HIF-1α signals due to mesangiolysis. Magnification, *200 (J).

Fig. 3. Semiquantitative analysis of morphologic changes in our glomerulonephritis model. The main lesion in the H+A group is initially detected on day 2 as mesangiolysis in glomeruli; however, there are no tubular lesions of necrosis except for tubular casts; in contrast, there are no morphological changes in the N and A groups. MES, Mesangiolysis score.

Fig. 4. Serum UN, Cr and SBP are increased with the combination of HV and AII. The serum UN (A) and Cr (B) levels in the H+A group on day 2 are significantly higher than other groups. SBP increases significantly with administration of AII (A and H+A groups) (C).

Fig. 5. The protein level of HIF-1α is increased by administration of HV and AII, and pretreatment of CoCl₂ increases HIF-1α expression before development of GN. HIF-1α is not detected in the N and HV groups (Day2). However, HIF-1α is detected in A (Day2) and H+A (Days 1 and 2) groups (A). The CoCl₂ group, in accord with the level of HIF-1α induction, was divided into two groups. HIF-1α is greatly induced before the development of GN (CoCl₂ group Pre-1), and is followed by a high level (CoCl₂ group Day2-1); in contrast, it is not efficiently induced (CoCl₂ group Pre-2), and also is scarcely detected on day 2 (CoCl₂ group Day2-2) (B). The rate of pre-induction of HIF-1α by CoCl₂ is comparable with that of the inhibition of GN by CoCl₂ (C).

Fig. 6. Pretreatment with CoCl₂ attenuates GN. Serum UN (A) and Cr (B) levels in the CoCl₂ group on day 2 are significantly decreased compared to those in the non-CoCl₂ group. There is no significant difference in SBP between the CoCl₂ and non-CoCl₂ groups (C).
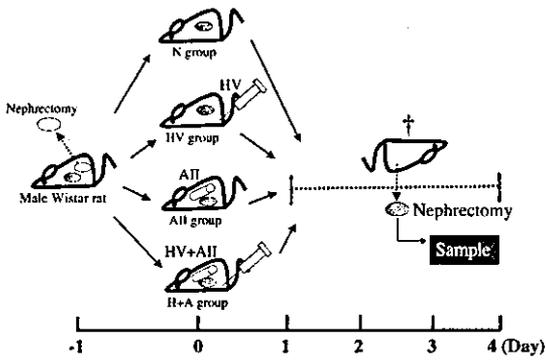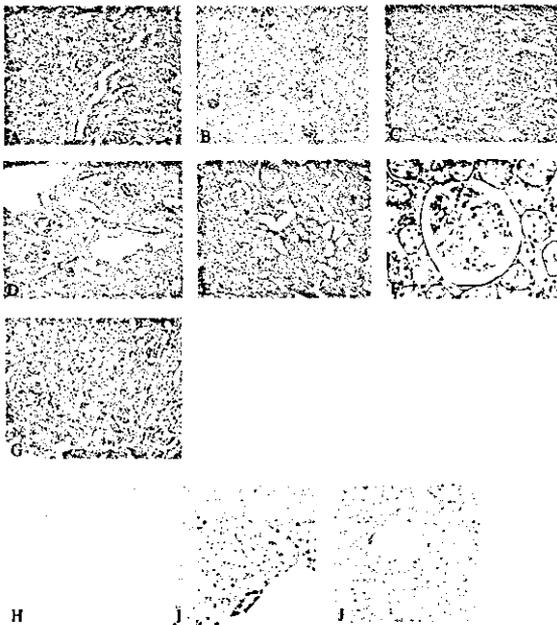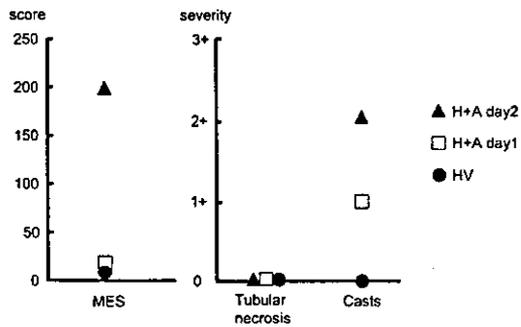
Fig. 1

Fig. 2

Fig. 3

Fig. 3

Fig. 4

Fig. 5